

Reliable measurements of the Seebeck coefficient on a commercial system

Yintu Liu, Chenguang Fu, Hanhui Xie, Xinbing Zhao, and Tiejun Zhu^{a)}

State Key Laboratory of Silicon Materials and Department of Materials Science and Engineering, Zhejiang University, Hangzhou 310027, China

(Received 15 January 2015; accepted 10 July 2015)

The Seebeck coefficient is an important parameter of thermoelectric materials, which is routinely measured by commercial or home-made equipment based on different methods. However, due to various temperature offsets in the measurement, the determination of temperature gradient can be inaccurate, leading to a large uncertainty in Seebeck coefficient. To elucidate the influence of the inaccurate temperature gradient on the determination of Seebeck coefficient, an error analysis has been performed on a commercial system. Several potential factors that may affect the establishment of temperature gradient were discussed in detail. A comparison between the single point method and the slope method was made to verify which is more accurate to calculate the Seebeck coefficient from the raw measurement data. It is suggested that the slope method is more preferable and the single point method can also be accurate enough when a relatively large temperature gradient is adopted.

I. INTRODUCTION

Thermoelectric (TE) materials, which can generate electricity from waste heat or be used as solid-state Peltier coolers, have attracted renewed attention because of their potential role in a global sustainable energy solution. The efficiency of a TE material is represented by the dimensionless figure of merit $zT = \alpha^2 \sigma T / \kappa$, which is usually obtained from the separate measurement of temperature T dependent Seebeck coefficient α , electrical conductivity σ , and thermal conductivity κ .^{1,2} Given the fact that a 20% improvement in the zT value of the state-of-the-art TE materials would make significant commercial impact, measurement accuracy is of critical importance. For example, compared to the values obtained today, a 30% overestimation of the high temperature thermal conductivity of the lead chalcogenides is found in the early steady-state method, leading to an underestimation of zT .^{3,4} Similarly, due to the various challenges in the measurements, a combined uncertainty of the power factor $\alpha^2 \sigma$ can readily reach up to 27%.⁵ Such discrepancies are to be expected even today as absolute accuracy in TE measurements is still not possible. Thus, sufficient care on the TE measurement should be taken, even if carried on commercial systems.⁶

The Seebeck coefficient is an important parameter of TE materials, which is routinely measured by different commercial or home-made instruments.^{7–10} However,

due to various techniques applied in the measurement and the absence of standardized criteria, the measured Seebeck coefficient is often subject to irreproducibility and inconsistency in results, making it difficult for interlaboratory comparison. Fortunately, a recent review gave a systemic comparison of a variety of metrologies applied on the Seebeck coefficient measurements, which provides convenience to the researchers in this field.¹¹

While it is not geometry dependent for isotropic materials, the Seebeck coefficient is highly sensitive to the electronic structure and thus can be a useful tool in the studies of transport properties of charge carriers. Recent progresses in modeling TE transport process have provided a powerful analytical tool to investigate TE materials and can be used to guide the optimization of TE efficiency.^{12–15} However, the outcome of the modeling is closely related to the experimentally measured TE parameters. For example, in the widely used single parabolic band model, the density of state effective mass m^* is calculated based on the experimental data of Seebeck coefficient and carrier concentration. Consequently, the incorrect measurement of the latter will cause a deviation from true m^* , which may lead to confusions, rather than boost the understanding of carrier transport features.

Based on the assumptions of differential technique, the Seebeck coefficient can be expressed as follow:

$$\alpha_{ab} = \frac{\Delta V_{ab}}{\Delta T}, \quad (1)$$

Where ΔV_{ab} is the electric potential between two different materials a and b, and $\Delta T = T_2 - T_1$ is the applied

Contributing Editor: Terry M. Tritt

^{a)}Address all correspondence to this author.

e-mail: zhutj@zju.edu.cn

DOI: 10.1557/jmr.2015.218

temperature difference. Note that the above formula is valid only when $\Delta T/T_{\text{ave}} \ll 1$, and T_{ave} is equal to $(T_2 - T_1)/2$.¹¹ From the definition, to obtain the Seebeck coefficient of an individual material, an additional correction to α_{ab} is necessary: $\alpha_{ab} = \alpha_b - \alpha_a$, where α_a is the Seebeck coefficient of the sample being measured and α_b is the Seebeck coefficient of the reference material.

Despite the simple conception, there are particular challenges in Seebeck coefficient measurement. The main challenge is to obtain accurate temperature gradient across the sample, which can be influenced by the thermal contact condition between the thermocouples and the sample surface. Both 2-point and 4-point measurements, as the currently dominant measurement geometries, fail to obviate the thermal contact resistance absolutely,^{16,17} which may disturb the determination of Seebeck coefficient, especially when the applied temperature difference is relatively small. Meanwhile, the temperature gradient must be controlled to avoid deviation from the constraint condition of Eq. (1). Therefore, the adoption of an appropriate temperature gradient is crucial to the certainty of the results, which may not be easily accessed for new researchers in this field. In addition, a variety of temperature gradients associated with different experimental techniques were applied in the literature, which caused more confusions.^{7,18,19}

In this study, we focus on error analysis for Seebeck coefficient measurement based on commercially available system and elucidate the influence of the inaccurate temperature gradient on the determination of Seebeck coefficient. Several potential factors that may affect the establishment of temperature gradient are discussed in detail. Based on a multiple ΔT method, we compare two different ways to extract the Seebeck coefficient from the raw measurement data. The slope method is proved to be more preferable to get a convincing result, while the single point method is also available when large temperature gradient is adopted. The present work demonstrates that, even using commercial system, the special care should be taken to guarantee the correctness of the measurement.

II. EXPERIMENTAL PROCEDURE

The measurements were performed on a commercial Linseis LSR-3 system equipped with an infrared furnace. The Seebeck coefficient was measured using a differential steady-state technique. The uncertainty of the Seebeck coefficient measurement for the Linseis system is claimed to be $\pm 5\%$ at room temperature. Several samples of typical TE materials, such as Bi_2Te_3 , PbTe , and ZrNiSn half-Heusler compounds were selected for the measurements. The samples were cut into bars with an identical dimension $2 \text{ mm} \times 2 \text{ mm} \times 12 \text{ mm}$.

A schematic diagram of the measurement system is presented in Fig. 1. The sample is mounted between two

platinum electrodes and held in place with pressure. To improve thermal and electrical contact, a thin graphite foil is utilized between the sample and each electrode, which can also act as a barrier to prevent possible chemical reactions between the sample and the platinum electrode. Two pairs of Pt-Pt + 10% Rh standard thermocouples are used to measure the temperature difference and associated voltage between them. Spring-driven contacts are also used for contacting the thermocouples to the sample. The entire length of the thermocouple is embedded in a twin bore alumina sheathing to avoid strain and contamination. Given the sample length, a value of 6 mm is selected as the probe spacing to ensure a uniform electrical conduction profile within the sample.¹¹ All the measurements are carried out in helium atmosphere at an overpressure of approximate 150 mBar, which is created after purging the system several times. Prior to any measurements, the apparatus was calibrated by measuring the Seebeck coefficient as a function of temperature on a constantan reference sample.

The average sample temperature is controlled by the infrared furnace. After the furnace has fully stabilized, an additional power is supplied from the lower electrodes to gain a temperature difference between the upper and lower electrodes, labeled as ΔT_E . The magnitude of ΔT_E can be preset by commercial testing software. Usually, a series of different ΔT_E is implemented at each temperature, i.e., the multiple temperature gradient method. The corresponding electric voltage ΔU_P and temperature gradient ΔT_P between two probe thermocouples can be measured sequentially in seconds. According to Eq. (1), the Seebeck coefficient of the sample can be obtained by,

$$\alpha_A = \frac{\Delta U_P}{\Delta T_P} - \alpha_{\text{Pt}} \quad , \quad (2)$$

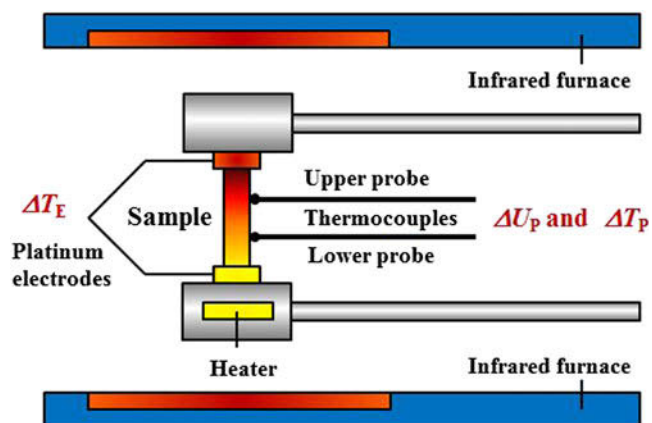


FIG. 1. Schematic diagram of the commercial Seebeck coefficient measurement apparatus.

Where α_A is the Seebeck coefficient of the sample being measured, α_{Pt} stands for the tabulated Seebeck coefficient of Pt wires (only the Pt legs of each Pt/Pt-10% Rh thermocouples are used for the ΔU_P measurement).

Based on the commercial system, there are two frequently used ways to extract the Seebeck coefficient from the raw measurement data, i.e., the single point method and the slope method. As for the former, the Seebeck coefficient is derived from a single voltage/temperature gradient pair based on the definition of Seebeck coefficient [Eq. (2)]. While the slope method often calculates the Seebeck coefficient from the linear fit of multiple electric voltage/temperature gradient data points rather than one.

III. RESULTS AND DISCUSSION

Up to date, commercial standard samples with properties close to the typical values of TEs are still not available for Seebeck coefficient measurements. It is therefore recommended that laboratories develop internal standards to identify instrument drift and valid the results. Half-Heusler alloy samples, in which we have rich experience,^{12,14,20} are used in our case due to their good mechanical properties and high thermal stability. An abnormal behavior of temperature gradient dependence of Seebeck coefficient was observed during periodical calibration measured using the single point method, as shown in Fig. 2(a). The Seebeck coefficient increases with decreasing ΔT_E , while the datasets obtained at large ΔT_E ($\Delta T_E = 32, 36, 40$ K) show a good agreement with each other. In addition, the deviations of the measured points at each environmental temperature obtained under small ΔT_E are more obvious. A further examination on the ΔT_P is presented in Fig. 2(b). As shown, a small ΔT_E leads to a small ΔT_P . Taking $\Delta T_E = 10$ K for example, the corresponding ΔT_P is as low as 0.5 K around 600 K. Thus, the measured Seebeck coefficient will have large fluctuation when the random

system error is in the same order of magnitude. The effects can be expressed as

$$\alpha_{A,\text{non-ideal}} = \frac{\Delta U_P + \delta \Delta U_P}{\Delta T_P + \delta \Delta T_P} - \alpha_{Pt} \quad (3)$$

Here, $\delta(\Delta U_P)$ is the spurious voltages that affect the ΔU_P reading, $\delta(\Delta T_P) = T_{\text{Lower}} - T_{\text{Upper}}$ is the temperature difference in the two thermocouple readings if they are at identical temperature. Under the assumption that both voltage and temperature offsets are constant, we can thus deduce that small temperature gradient will contribute to larger relative error, while large temperature gradient succeeds in minimizing the influence of offsets due to the larger voltage signals and denominator.

It is noteworthy that both voltage and temperature offsets cannot be detected directly during the measurement. And also, these offsets are strongly dependent on the contacts, measurement techniques, and the thermocouple conditions. The reported voltage offsets can range from a few μV up to almost 1 mV.^{10,11,16} Due to its high sensitivity to the thermocouple conditions, the temperature offsets are more prone to arise: firstly, real thermocouples are not chemically or physically homogenous and the typical accuracy of a thermocouple reading is on the order of 1 K, at best ~ 0.2 K. As mentioned above, the probe thermocouples are attached directly to the sample. A chemical reaction frequently occurs at the contact point, together with the thermal aging, leading to a quicker degradation of the thermocouples. Moreover, the thermocouples can draw heat away from the sample, causing a temperature deviation from the real sample temperature (known as the ‘‘cold finger effect’’^{5,6}).

Other factors not included above may as well make a contribution to the voltage offsets and temperature offsets. With the aim to increase the reliability of the measurement procedure, it is necessary to give a full evaluation on these factors and thus find ways to eliminate the offsets as far as possible. However, it is

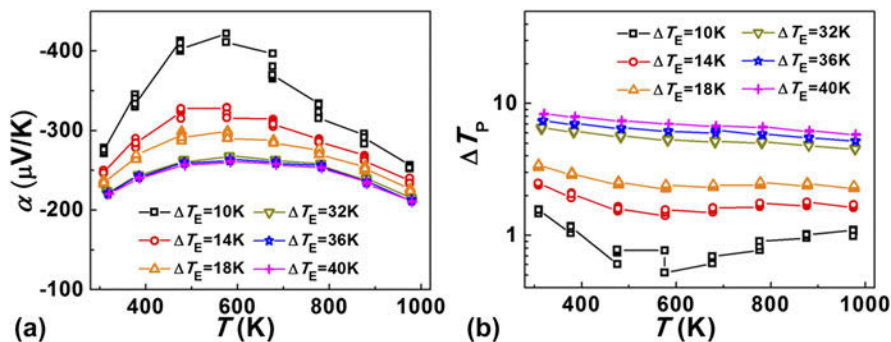


FIG. 2. Effect of different ΔT_E on (a) the seebeck coefficient and (b) ΔT_P for a typical ZrNiSn half-Heusler compound. Small ΔT_E leads to small ΔT_P , as a result, the measured Seebeck coefficient will have large fluctuation due to the random system error.

difficult to identify all the factors explicitly during the measurement from the point of view of stochastic effect. Additionally, some of the offsets are relevant to the intrinsic drawbacks of the applied measurement technique and instrument design, which cannot be readily eliminated at present. On such occasion, it is the second-best choice to seek strategies to minimize the influence of the ubiquitous offsets on the final determination of the Seebeck coefficient, e.g., large temperature gradient and effective data analysis methods.

Inspired by the integral method adopted in early days,²¹ a relatively large temperature gradient has a benefit in minimizing the influence of voltage offsets due to

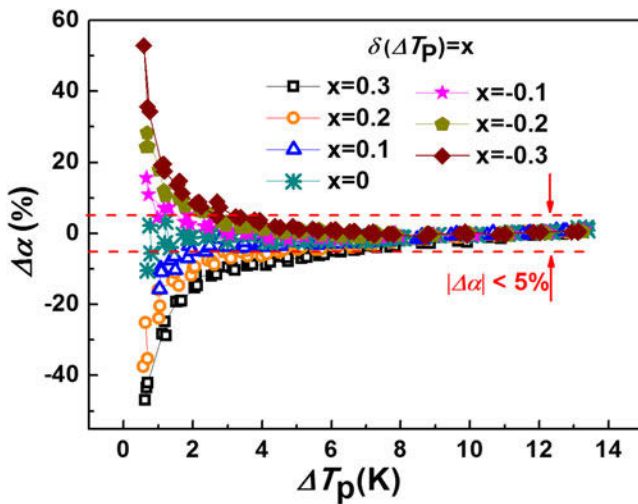


FIG. 3. The effect of ΔT_p on the measured Seebeck coefficient at room temperature when artificially enlarging the random system error for a typical ZrNiSn half-Heusler compound.

TABLE I. The minimum ΔT_p and ΔT_E required to fulfill $|\Delta\alpha| < 5\%$ at different $\delta(\Delta T_p)$ at 300 K for half-Heusler TE materials.

$\delta(\Delta T_p)/K$	-0.3	-0.2	-0.1	0	0.1	0.2	0.3
$\Delta T_p/K$	3.3	2.9	1.8	0.8	2.4	4.5	5.9
$\Delta T_E/K$	14.0	12.0	8.0	4.0	10.0	18.0	24.0

the large voltage signals. The same effect is expected in the differential steady-state method, as presented in Eq. (3). To verify this effect experimentally, further tests were carried out. Experiments were conducted at 300 K on a ZrNiSn half-Heusler compound. Different temperature offsets $\delta(\Delta T_p)$ [$\delta(\Delta T_p) = -0.3, -0.2, -0.1, 0, 0.1, 0.2, 0.3$ K] were deliberately introduced by making different cold junction temperature compensations for the two probe thermocouples. That can be realized through the corresponding software in the commercial Linseis instrument. We would like to emphasize that the true temperature offsets are not the ones used here, but a combination of $\delta(\Delta T_p)$ and the undetectable temperature offsets during the measurement. As the temperature gradient between electrodes (ΔT_E) varies from 4 to 50 K by the step of 2 K, the resulting temperature gradient (ΔT_p) and electric voltage (ΔU_p) between probe thermocouples is measured. At each temperature gradient, three electric voltages are measured for consistency check.

Figure 3 shows the deviation of the Seebeck coefficient at room temperature versus ΔT_p with different temperature offsets $\delta(\Delta T_p)$. The deviation is characterized quantitatively by the percent error,

$$\Delta\alpha = \frac{|\alpha_{\text{measured}}| - |\alpha_{\text{convergence}}|}{|\alpha_{\text{convergence}}|} \times 100\% \quad (4)$$

Here, $\alpha_{\text{convergence}}$ is the convergence value obtained at large ΔT_p , which is considered as the true sample Seebeck coefficient. This will be proved to be reasonable later. It can be seen that the error decreases quickly with increasing the temperature gradient. When $\delta(\Delta T_p) < 0$ (filled symbols), the calculated uncertainties are all higher than zero, suggesting an overestimation of the Seebeck coefficient. Conversely, an underestimation for $\delta(\Delta T_p) > 0$ (open symbols). This is supported by Eq. (3). For any fixed value of ΔT_p , the error increases with increasing the $|\delta(\Delta T_p)|$. In other words, the larger the temperature offset is, the larger temperature gradient is needed to keep the error under an

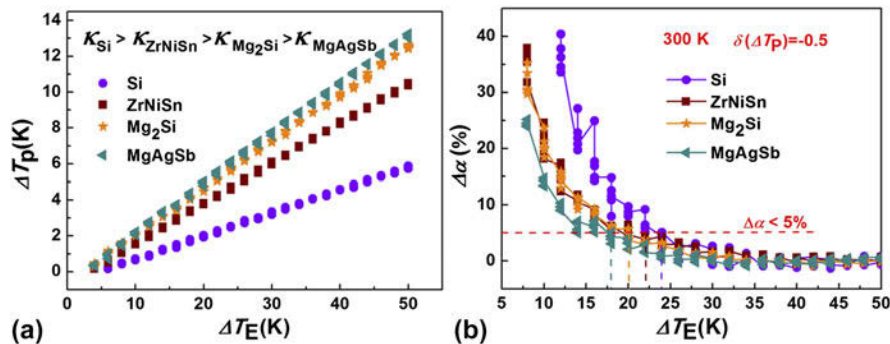


FIG. 4. ΔT_E dependence of (a) ΔT_p and (b) $\Delta\alpha$ for materials with different thermal conductivity. The temperature offset $\delta(\Delta T_p)$ is set as -0.5 K.

acceptable level. Generally, a variation of about 5% in measured Seebeck coefficient can be accepted at room temperature. With this criterion, the required minimum temperature gradients for both electrodes and probe thermocouples are listed in Table I. We further observed that the three data points measured at the same temperature gradient show different degrees of fluctuation, even for $\delta(\Delta T_P) = 0$ when the temperature gradient $\Delta T_P < 1$. This gives an indication that other sources of voltage or temperature offsets may probably exist. The effect of these offsets on the determination of Seebeck coefficient can be exaggerated when a small temperature gradient is used. In contrast, a large temperature gradient makes it possible to get a relatively convincing result in the presence of small system offsets.

Being aware of the necessity to maintain a relatively large temperature gradient throughout the whole measurement, we should pay another attention to the potential

TABLE II. The minimum ΔT_E and ΔT_P required to fulfill $|\Delta\alpha| < 5\%$ for different materials at 300 K. The temperature offset $\delta(\Delta T_P)$ is set as -0.5 K.

Materials	Si	FeVSb	ZrNiSn	PbTe	Mg ₂ Si	Bi ₂ Te ₃	MgAgSb
$\kappa/W \text{ m}^{-1} \text{ K}^{-1}$	62	10	8	2.5	1.8	2.0	1.0
$\Delta T_P/\text{K}$	2.5	3.8	4.2	4.5	4.7	4.5	4.3
$\Delta T_E/\text{K}$	24	20	22	20	20	20	18

factors that may affect the establishment of the temperature gradient. From our previous experience, when the same value of the temperature difference between electrodes (ΔT_E) is supplied via the program setting, the obtained temperature gradient between probe thermocouples (ΔT_P) varies among different materials, or more precisely, depends on the thermal conductivity of the measured material, as shown in Fig. 4(a). Here, four typical TE materials with quite different thermal conductivity ($\kappa_{\text{Si}} > \kappa_{\text{ZrNiSn}} > \kappa_{\text{Mg}_2\text{Si}} > \kappa_{\text{MgAgSb}}$) are tested at room temperature. All other conditions including sample dimension keep the same. It can be seen that the ΔT_P increases linearly with increasing the ΔT_E , indicating a linear temperature gradient distribution within the sample. For any ΔT_E , a smaller ΔT_P is obtained by a higher thermal conductivity material, suggesting that it is harder to establish a temperature gradient across the sample. Thus, the Si material is apt to get a larger error compared to the MgAgSb material if the same value of offset exists in the instrument, as illustrated in Fig. 4(b). To keep the error under a widely accepted level, a larger ΔT_E is needed for Si material accordingly. Other typical TE materials were also tested at room temperature. The minimum ΔT_E and ΔT_P required to fulfill $|\Delta\alpha| < 5\%$ are tabulated in Table II.

Another widely concerned factor which plays an important role in the determination of temperature gradient refers to the heat loss. Figure 5(a) represents the ΔT_P

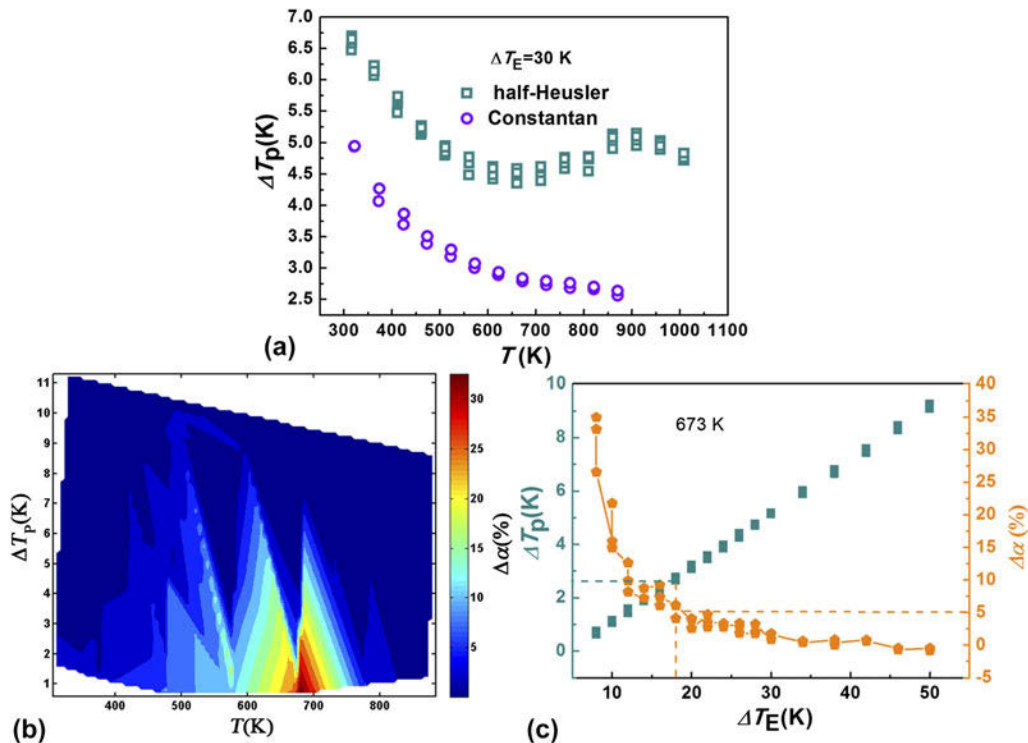


FIG. 5. (a) Temperature dependence of ΔT_P when using a constant ΔT_E for ZrNiSn half-Heusler compound and Constantan. (b) Percent error of the measured Seebeck coefficient as a function of both furnace temperature and ΔT_P . (c) ΔT_E dependence of $\Delta\alpha$ and ΔT_P at 673 K.

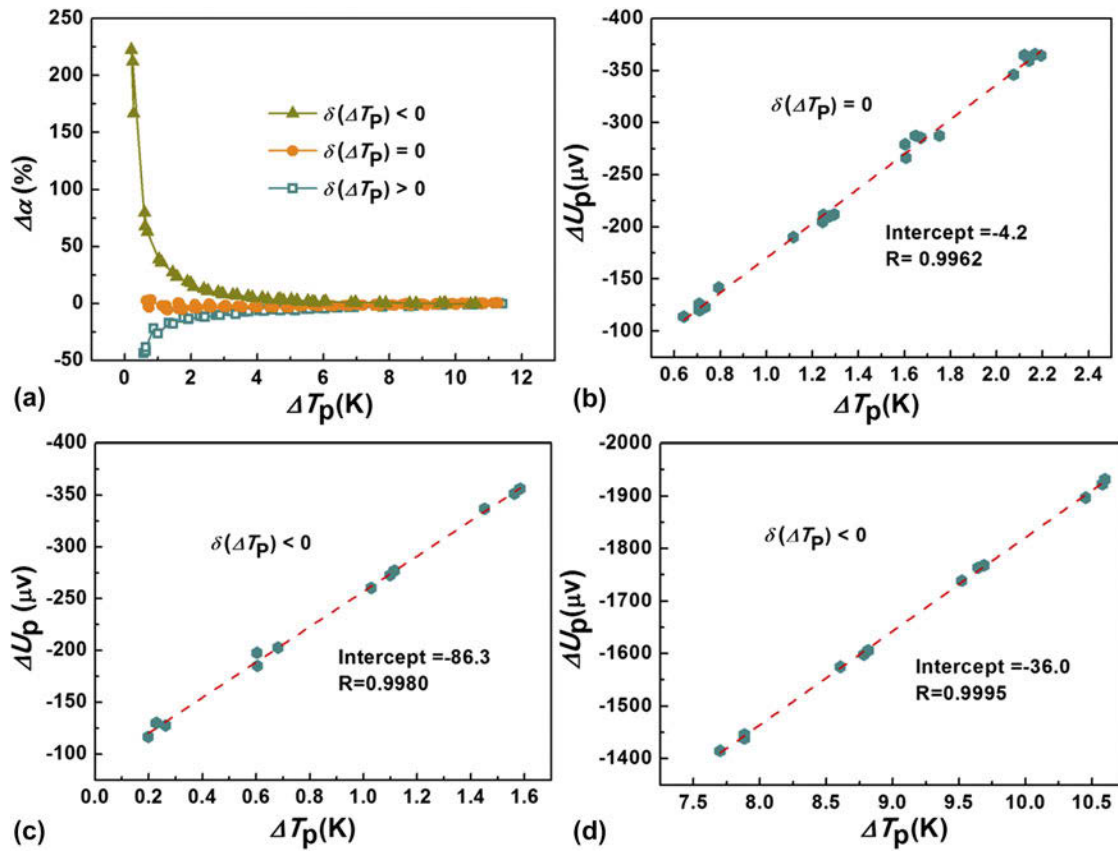


FIG. 6. (a) Percent error of the measured Seebeck coefficient as a function of ΔT_P by the single point method when artificially changing the random system error. (b), (c), and (d) Electric voltage between probe thermocouples ΔU_P versus ΔT_P .

as a function of furnace temperature for two different materials, i.e., constantan and ZrNiSn compound. As shown, even though the temperature difference between electrodes (ΔT_E) is kept constant throughout the whole measured temperature range, the resulting ΔT_P varies obviously. For constantan, the ΔT_P decreases monotonously with increasing the furnace temperature. At room temperature, a ΔT_P value of 5.0 K can be achieved, while high temperature results in a much smaller one ($\Delta T_P = 2.5$ K at 875 K). This can be attributed to the large lateral radiation at high temperature. As a result, the temperature difference between the two ends of the sample is not exactly the ΔT_E detected at two electrodes, but a smaller one. A roughly similar temperature dependence was observed in ZrNiSn half-Heusler sample. The small difference at high temperatures can be considered as the contributions from different thermal conductivity and thermal emissivity.

The deviation of the Seebeck coefficient as a function of both furnace temperature and ΔT_P is plotted in Fig. 5 (b). The measurement was carried on a ZrNiSn sample with the $\delta(\Delta T_P) = 0$. At each furnace temperature, the temperature gradient between electrodes (ΔT_E) is set from 8 to 50 K. It is surprising that a large error arises around

TABLE III. The Seebeck coefficients calculated from slope method and single point method at different temperature offsets $\delta(\Delta T_P)$ when $\Delta T_P < 2$ K.

	$\delta(\Delta T_P) = 0$	$\delta(\Delta T_P) < 0$
Single point method/ $\mu\text{V K}^{-1}$	-169.7	-200 to -300
Slope method/ $\mu\text{V K}^{-1}$	-166.1	-170.8

700 K where a minimum ΔT_P is obtained. The result of further analysis is shown in Fig. 5(c). According to what we have analyzed above, the behavior of the percent error versus ΔT_E indicates that some random offsets arise during the measurement, and the $\delta(\Delta T_P)$ is supposed to be negative. Though some offsets arise, a ΔT_E value larger than 20 K can still make it possible to meet the requirement of $|\Delta\alpha| < 5\%$. It is therefore advisable to adopt a relatively large temperature gradient to minimize the influence of the offsets on the determination of Seebeck coefficient.

All the above data analyses are based on the single point method. Usually, the slope method, which calculates the Seebeck coefficient from the slope of linear fit of multiple electric voltage/temperature gradients, is

TABLE IV. The Seebeck coefficient calculated from two different methods when a large ΔT_P ($5 \text{ K} < \Delta T_P < 10 \text{ K}$) is adopted. The measurement is carried at room temperature.

Materials	Si	FeVSb	ZrNiSn	PbTe	Mg ₂ Si	Bi ₂ Te ₃	MgAgSb
Single point method/ $\mu\text{V K}^{-1}$	-120.7	139.8	-205.5	130.5	-165.8	-148.7	-190.6
Slope method/ $\mu\text{V K}^{-1}$	-125.2	141.1	-203.9	132.8	-165.1	-147.8	-190.2

more widely used in steady-state measurement. To investigate which method is the better way to extract the Seebeck coefficient from the raw measurement data, a comparison is made between these two methods. The data shown in Fig. 6 are collected at 300 K from one ZrNiSn half-Heusler sample. Figure 6(a) shows a representative result of the single point method which has been discussed in detail in Fig. 3, while Figs. 6(b)–6(d) represent the slope method with the measured Seebeck coefficient $\alpha = -171 \pm 3\% \mu\text{V K}^{-1}$. The intercept shown here can be interpreted as a electric voltage offset due to nonideal contact condition. Also given in the figures is the linear correlation coefficient R of the linear fit, which can be used to judge the quality of the measurement. Under the condition that a small ΔT_P is adopted ($\Delta T_P < 2 \text{ K}$), The Seebeck coefficients calculated both from the single point method and the slope method are listed in Table III. We can see that the results are in a good agreement with each other if the offset is small. In contrast, when a large offset is introduced, the slope method can still obtain a rather reasonable value while the single point method results in a large error. Comparing the intercept and voltage signals in Fig. 6(d) with those in Fig. 6(c), we can find again that a relatively large ΔT_P is preferable for single point method due to a smaller relative error. The listed in Table IV are the Seebeck coefficients calculated from two different methods when a large ΔT_P ($5 \text{ K} < \Delta T_P < 10 \text{ K}$) is adopted. It can be seen that a good agreement was obtained between the two datasets.

IV. CONCLUSIONS

An error analysis has been performed on a commercial Seebeck coefficient measurement system. Due to sources of temperature offsets in the measurement, the determination of temperature gradient can be inaccurate, leading to a large error in Seebeck coefficient. To quantitatively investigate the effect of the temperature offsets on the Seebeck coefficient, additional temperature offsets have been deliberately induced by making different cold junction temperature compensation for the two probe thermocouples. The results indicate that large temperature gradient is preferable to force this error to an acceptable level for single point method. Comparing to the single point method, the slope method is more accurate to calculate the

Seebeck coefficient from the raw measurement data. A good agreement between these two methods can be achieved when a relatively large temperature gradient ($5 \text{ K} < \Delta T_P < 10 \text{ K}$) is applied in the measurement. Several potential factors, such as the thermal conductivity of the sample, sample temperature, and thermal emissivity, may have an influence on the establishment of ΔT_P . Thus, to make sure ΔT_P falls in the range mentioned above, additional attention should be taken when the temperature control program is set up.

In the four-point geometry, the two probe thermocouples are directly attached to the sample, and chemical reactions are expected to occur at the contact point, leading to degradation of the thermocouples. Therefore, frequent device calibration and probe thermocouple replacement are necessary for regular maintenance.

ACKNOWLEDGMENTS

The work was supported by the National Basic Research Program of China (2013CB632503), the Nature Science Foundation of China (51171171), the Program for New Century Excellent Talents in University (NCET-12-0495), and the Program for Innovative Research Team in University of Ministry of Education of China (IRT13037).

REFERENCES

1. T.M. Tritt: Holey and unholey semiconductors. *Science* **283** (5403), 804 (1999).
2. G.J. Snyder and E.S. Toberer: Complex thermoelectric materials. *Nat. Mater.* **7**(2), 105 (2008).
3. H. Wang, Y. Pei, A.D. LaLonde, and G.J. Snyder: Heavily doped p-type PbSe with high thermoelectric performance: An alternative for PbTe. *Adv. Mater.* **23**(11), 1366 (2011).
4. H. Wang, Y. Pei, A.D. LaLonde, and G.J. Snyder: Weak electron-phonon coupling contributing to high thermoelectric performance in n-type PbSe. *Proc. Natl. Acad. Sci.* **109**(25), 9705 (2012).
5. J. Mackey, F. Dynys, and A. Sehirlioglu: Uncertainty analysis for common Seebeck and electrical resistivity measurement systems. *Rev. Sci. Instrum.* **85**(8), 085119 (2014).
6. K.A. Borup, J. de Boor, H. Wang, F. Drymiotis, F. Gascoin, X. Shi, L. Chen, M.I. Fedorov, E. Müller, and B.B. Iversen: Measuring thermoelectric transport properties of materials. *Energy Environ. Sci.* **8**(2), 423 (2015). doi:10.1039/c0xx00000x.
7. Z. Zhou and C. Uher: Apparatus for Seebeck coefficient and electrical resistivity measurements of bulk thermoelectric materials at high temperature. *Rev. Sci. Instrum.* **76**(2), 023901 (2005).
8. C. Wood, D. Zoltan, and G. Stapfer: Measurement of Seebeck coefficient using a light pulse. *Rev. Sci. Instrum.* **56**(5), 719 (1985).

9. A. Guan, H. Wang, H. Jin, W. Chu, Y. Guo, and G. Lu: An experimental apparatus for simultaneously measuring Seebeck coefficient and electrical resistivity from 100 K to 600 K. *Rev. Sci. Instrum.* **84**(4), 043903 (2013).
10. J. Martin: Apparatus for the high temperature measurement of the Seebeck coefficient in thermoelectric materials. *Rev. Sci. Instrum.* **83**(6), 065101 (2012).
11. J. Martin, T. Tritt, and C. Uher: High temperature Seebeck coefficient metrology. *J. Appl. Phys.* **108**(12), 121101 (2010).
12. H. Xie, H. Wang, Y. Pei, C. Fu, X. Liu, G.J. Snyder, X. Zhao, and T. Zhu: Beneficial contribution of alloy disorder to electron and phonon transport in half-Heusler thermoelectric materials. *Adv. Funct. Mater.* **23**(41), 5123 (2013).
13. Y. Pei, A.D. LaLonde, H. Wang, and G.J. Snyder: Low effective mass leading to high thermoelectric performance. *Energy Environ. Sci.* **5**(7), 7963 (2012).
14. C. Fu, T. Zhu, Y. Pei, H. Xie, H. Wang, G.J. Snyder, Y. Liu, Y. Liu, and X. Zhao: High band degeneracy contributes to high thermoelectric performance in p-type half-Heusler compounds. *Adv. Energy Mater.* **4**(18), 1400600 (2014).
15. C. Fu, T. Zhu, Y. Liu, H. Xie, and X. Zhao: Band engineering of high performance p-type FeNbSb based half-Heusler thermoelectric materials for figure of merit $zT > 1$. *Energy Environ. Sci.* **8**(1), 216 (2014).
16. S. Iwanaga, E.S. Toberer, A. LaLonde, and G.J. Snyder: A high temperature apparatus for measurement of the Seebeck coefficient. *Rev. Sci. Instrum.* **82**(6), 063905 (2011).
17. J. Martin: Protocols for the high temperature measurement of the Seebeck coefficient in thermoelectric materials. *Meas. Sci. Technol.* **24**(8), 085601 (2013).
18. V. Ponnambalam, S. Lindsey, N.S. Hickman, and T.M. Tritt: Sample probe to measure resistivity and thermopower in the temperature range of 300-1000 K. *Rev. Sci. Instrum.* **77**(7), 073904 (2006).
19. A.T. Burkov, A. Heinrich, P.P. Konstantinov, T. Nakama, and K. Yagasaki: Experimental set-up for thermopower and resistivity measurements at 100-1300 K. *Meas. Sci. Technol.* **12**(3), 264 (2001).
20. C. Yu, T. Zhu, R. Shi, Y. Zhang, X. Zhao, and J. He: High-performance half-Heusler thermoelectric materials $\text{Hf}_{1-x}\text{Zr}_x\text{NiSn}_{1-y}\text{Sb}_y$ prepared by levitation melting and spark plasma sintering. *Acta Mater.* **57**(9), 2757 (2009).
21. C. Wood, A. Chmielewski, and D. Zoltan: Measurement of Seebeck coefficient using a large thermal gradient. *Rev. Sci. Instrum.* **59**(6), 951 (1988).